

THE STATIC THRUST CHARACTERISTICS OF A PROPELLER
WITH TRAILING-EDGE FLAPS

A THESIS

Submitted in partial fulfillment
of the requirements for the Degree
of Master of Science in Aeronautical Engineering

by

Donnell W. Dutton

Georgia School of Technology
Atlanta, Georgia
1940

N 8 Jul 40

52010

Approved:

Acknowledgements

The writer wishes to thank Professor Montgomery Knight for his assistance in planning the attack on the problem and for his very helpful criticisms throughout its development; and Professor A. M. Schwartz and Mr. R. H. Fagan for their help and criticisms.

TABLE OF CONTENTS

	Page
Approval Sheet.....	ii
Acknowledgments.....	iii
Summary.....	1
Introduction.....	1
Design of Propeller Used in This	
Analysis.....	3
Results and Discussion.....	6
Conclusions.....	11
References.....	13

TABLES

FIGURES

THE STATIC THRUST CHARACTERISTICS OF A PROPELLER
WITH TRAILING-EDGE FLAPS

Summary

The analytical investigation presented in this paper was made to determine whether the static thrust of a propeller, and consequently the take-off and climb of an airplane, could be improved by providing the trailing edge of the propeller blades with flaps to effect the necessary pitch changes.

A comparison is made between the fixed-pitch propeller, the conventional variable-pitch propeller, wherein the pitch is changed by rotating the blade at the hub, and the propeller equipped with trailing-edge flaps. It is shown that the static thrust of a propeller can be increased by the use of flaps, and that this increase is approximately 44 per cent of the increase obtained from the conventional variable-pitch propeller.

Introduction

The principle of hinging the trailing edge of a propeller blade to effect pitch changes, instead of turning the whole blade in the hub, is not new. Apparently, however, no theoretical or experimental analysis has ever been made of a propeller so equipped.

The idea was suggested to the writer by Walter Castles, a former graduate student, with the thought that it might be worked out quite cheaply for small aircraft propellers. Most of the light airplanes are already being made clean enough to take advantage of a variable-pitch propeller, but

none are available. This is due principally to the fact that the cost of producing a variable-pitch propeller of the conventional type, for a small motor, is so high, only a few attempts have been made to develop one. The French Ratier and Levasseur two-position propellers have been used successfully on several small racing planes, and the Everel propeller developed in this country is also a step in the right direction. Both types, however, are still too heavy and too expensive for general use.

Hinging the trailing edge of each blade allows the two-bladed propeller to be built straight through the hub as in present fixed-pitch wooden propellers. This type of construction would result in a considerable saving in weight over the present type of variable-pitch propeller; principally by eliminating the heavy hub that is normally required to house the operating mechanism as well as carry the full centrifugal load of the blades. The centrifugal load of a 20 per cent chord flap would be small, and could in all probability be carried by a piano-type hinge. Mass balancing and air load balancing also should not be difficult for a two-position propeller, that is, take-off and high-speed conditions, and could be worked out quite easily.

This paper has been limited to a mathematical analysis of the aerodynamic characteristics of a "flapped" propeller in the static thrust condition. The first of the two purposes was to determine whether any increase in static thrust could be realized by moving a flap to negative angles, thus permitting the propeller to "rev up" to full-throttle rated revolutions per minute on the ground. The second purpose was to compare the increase in thrust with that obtained by turning an unflapped blade in the hub as in the conventional variable-pitch propeller.

It is recognized, as pointed out in Ref.1, that static thrust is not an exact indication of the take-off characteristics. However, Ref.2 shows that

for lightly loaded propellers it can be taken as a fair criterion. Static thrust was used in this analysis because there is less labor involved in the calculation of the induced velocity parameter for the static-thrust condition than for the high-speed condition.

Design of the Propeller Used in the Analysis

The propeller used in these calculations was designed by Weick's Method outlined in Ref.3 to the following specifications:

Diameter, $D = 6$ ft.

Speed of rotation, $N = 2550$ r.p.m.; $n = 42.5$ r.p.s.

Velocity, $V = 126$ m.p.h.

Using these values, which are fairly representative of present light airplanes, the effective pitch $\frac{V}{nD}$ was found to be equal to 0.72.

The pitch diameter ratio, $\frac{P}{D} = 0.81$ was determined at the three-quarter radius from Fig. 10 of Ref.3. at the above value of $\frac{V}{nD} = 0.72$ for a high-speed airplane. Therefore

$$P = 0.81 \times 6 = 4.86 \text{ ft.}$$

This gave the geometric blade angle at the three-quarter radius for the particular airfoil used in Ref.3,

$$\theta_{.75} = \tan^{-1} \frac{4.86}{2\pi \frac{3}{4} R} = 19^\circ.$$

This angle was corrected to read from zero lift so that any airfoil could be used. Fig. 15, Ref. 4, shows the angle of attack for zero lift of the

ten per cent section used at the three-quarter radius of the standard propeller in Ref. 3 to be -4.4° . The absolute angle of attack is, therefore,

$$\theta_{.75} = 19^\circ - (-4.4^\circ) = 23.4^\circ$$

and the new aerodynamic pitch found to be

$$p' = 2\pi \frac{3}{4} R \tan 23.4^\circ = 6.12 \text{ ft.}$$

It should be noted that all angles of attack referred to in the remainder of this paper are measured from zero lift.

With this new pitch, the blade angles at the various propeller sections were determined for a constant-pitch propeller from the relationship

$$\theta_r^\circ = \tan^{-1} \frac{6.12}{2\pi r}$$

Table I shows the blade angles at the various stations along the blade, and also the geometric characteristics of the propeller as finally designed. Fig. 1a is a sketch of the blade planform and Fig. 1b is a typical cross-section of the blade showing the plain trailing-edge flap.

The N.A.C.A. M-6 airfoil section with a twenty per cent plain flap was used for the propeller and is described in detail in Ref. 5. The N.A.C.A. M-6 is not a conventional propeller section, but it is the only section that has been completely tested with up or negative flap angles, and has the data presented in a form suitable for use in this report. The data given in Tables I, II, III, and IV of Ref. 5, for α , C_L , and C_D were corrected to infinite aspect ratio by the use of Prandtl's formulae in

Ref. 6 as follows:

$$\alpha_o = \alpha - \frac{C_L}{\pi AR_e} (1 + \tau) \quad 57.3$$

$$C_{D_o} = C_D - \frac{C_L^2}{\pi AR_e} (1 + \sigma)$$

where

$AR_e = 7.318$ and is the effective aspect ratio from page 2, Ref. 4.

$$\tau = .2060 \quad (\text{Fig. 11, Ref. 6})$$

$$\sigma = .0675 \quad (\text{Fig. 11, Ref. 6})$$

whence

$$\alpha_o = \alpha - 3.01 C_L \quad (\text{Angle of attack for infinite aspect ratio})$$

$$C_{D_o} = C_D - .0464 C_L^2 \quad (\text{Profile drag coefficient}).$$

The corrected values are shown in Figs. 10 and 11. Fig. 10 is a plot of section lift coefficient, C_L versus the angle of attack for infinite aspect ratio, α_o , at the various up-flap angles, δ_f . Fig. 11 is a similar plot of profile drag coefficient, C_{D_o} versus α_o .

The propeller was assumed to have the same airfoil section at every point along the blade. This is, of course, an approximation, but if the section at the three-quarter radius is chosen as representative, as was done in this case, the approximation will fall within the desired accuracy.

Results and Discussion

Using a method of approximation outlined in Ref. 2, the following formulae will completely determine the characteristics of a propeller.

$$\phi = \frac{1}{2.06} \left[\left(\frac{\lambda_c}{x} - \frac{a_0}{4} \right) + \sqrt{\left(\frac{\lambda_c}{x} - \frac{a_0}{4} \right)^2 + 1.03 a_0 \theta_c} \right] \quad (1)$$

$$C_x = C_L \sin \phi + C_D \cos \phi$$

$$C_y = C_L \cos \phi + C_D \sin \phi$$

$$R \frac{dT_c}{dr} = \sigma \left(\frac{r}{R} \right)^3 C_y \sec^2 \phi$$

$$R \frac{dQ_c}{dr} = \sigma \left(\frac{r}{R} \right)^4 C_x \sec^2 \phi$$

where

$$\phi_c = \frac{\phi}{\sigma}$$

$$\theta_c = \frac{\theta}{\sigma}$$

$$\lambda_c = \frac{\lambda}{\sigma}$$

ϕ = induced angle

θ = blade angle (Measured from zero lift)

$$\lambda = \frac{V}{\pi n D} \quad (\text{Slip function})$$

$$\sigma = \text{blade element solidity} = \frac{bc}{2\pi r}$$

where

b = number of blades

c = chord of blade element

r = radius of element

$$a_0 = 5.21 \text{ (slope of lift curve, see Fig. 1).}$$

C_L and C_{D_0} are found from Figs. 10 and 11 at

$$\alpha_0 = \Theta - \phi.$$

For static thrust determination $\lambda = 0$ and the induced angle formula reduces to

$$\begin{aligned} \phi &= \frac{1}{2.06} \left[-\frac{a_0}{4} + \sqrt{\left(\frac{a_0}{4}\right)^2 + 1.03 a_0 \Theta_c} \right] \\ &= \frac{1}{2.06} \left[-1.30 + \sqrt{1.695 + 5.37 \Theta_c} \right]. \end{aligned} \quad (2)$$

The results obtained through the use of the above formulae are presented in Figs. 2 to 8 and TABLES II to VIII.

Figs. 2 and 3 are the thrust and torque grading curves for the fixed-pitch propeller in the high-speed condition, $\lambda = .23$, and the static-thrust condition, $\lambda = 0$, respectively. These curves were plotted using the tabulated values in TABLES II and III, the values having been obtained as follows: The induced velocity parameter, ϕ_c , was first determined for each station along the blade from the appropriate formula, that is, Eq. 1 was used for $\lambda = .23$ and Eq. 2 for $\lambda = 0$. The induced velocity angles ϕ could now be determined for each blade element, and when subtracted from the blade angle Θ , gave the angle of attack of the blade element at that station. Corresponding C_L and C_{D_0} values were found from the curves of Figs. 10 and 11 at $\delta_f = 0$, and the values used in the formulae for C_x and C_y . $\frac{r}{R}$ and Θ

having been determined previously, $R \frac{dT_c}{dr}$ and $R \frac{dQ_c}{dr}$ could then be calculated for each station and plotted as shown in Figs. 2 and 3.

The values in TABLES IV and V are plotted in Figs. 4 and 5 and are the static thrust and torque grading curves for the variable-pitch propeller with the blade angles reduced 5° and 10° respectively. The calculations for these curves were similar to the ones for Fig. 3, the only difference being that Θ at each blade section is now reduced 5° in TABLE IV and 10° in TABLE V. New ϕ values were obtained from Eq. 2 and the determination of $R \frac{dT_c}{dr}$ and $R \frac{dQ_c}{dr}$ followed directly, C_L and C_{D_0} values having been read from the curve for $\delta_f = 0$ as before.

The only difference in the calculations of the values of $R \frac{dT_c}{dr}$ and $R \frac{dQ_c}{dr}$ for the propeller with trailing-edge flaps was in the determination of Θ and the care that had to be taken in reading the values of C_L and C_{D_0} .

From Fig. 10 it can be seen that the angle of zero lift for the M-6 Section with flaps is less than for the section without flaps; 2.8° less with the flap raised 5° ($\delta_f = -5^\circ$); 4.9° less with the flap raised 10° ($\delta_f = -10^\circ$); and 7.5° for the flap raised 20° ($\delta_f = -20^\circ$). In the variable-pitch propeller turning the blade 5° in the hub causes Θ to change 5° all along the blade, but raising the flap 5° causes an effective change in Θ of only 2.8° . Likewise, raising the flap 10° reduces the effective Θ only 4.9° and for $\delta_f = -20^\circ$, Θ is reduced 7.5° .

The three new values of Θ resulting from the three flap settings were used in the determination of the static thrust and torque grading curves for the three propellers equipped with trailing-edge flaps.

ϕ was determined as before from Eq. 2 and the new values of Θ_c . α_0 could now be calculated from $\Theta - \phi$ as before. The C_L and C_{D_0} values were read from the appropriate curves remembering that α_0 is from the zero lift

of the effective section. An example is the calculation for the propeller with the flap raised 5° , ($\Theta_{.75} = 23.4 - 2.8 = 20.6^\circ$). Here, ϕ was equal to 7.5° and, therefore, $\alpha_o = 20.6 - 7.5 = 13.1^\circ$. This α_o should be read from the point B in Figs. 10 and 11, or it can be read from point A and the ordinates for $\delta_f = 0$ used by remembering to add 2.8° to each α_o found.

The results obtained from these calculations on the propeller with trailing-edge flaps are tabulated in TABLES VI, VII, and VIII. The corresponding thrust and torque grading curves are shown in Figs. 6, 7, and 8.

The results of the graphic integration of all the thrust and torque grading curves, Figs. 2 to 8 inclusive, are shown in TABLE IX. The areas thus obtained when multiplied by their respective integration constants gave Glauert's thrust coefficient, T_c , and torque coefficient, Q_c . These values are also listed in TABLE IX.

Total thrust, torque and powers were determined from Glauert's formulae in Ref. 7 as follows:

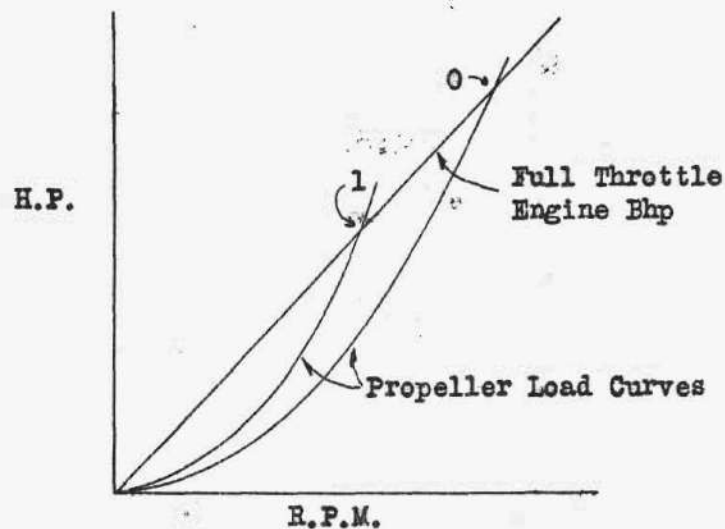
$$T = T_c \rho \pi R^4 \Omega^2 = .605 \Omega^2 T_c \text{ (lbs)}$$

$$Q = Q_c \rho \pi R^5 \Omega^2 = 1.815 \Omega^2 Q_c \text{ (ft.lbs)}$$

$$P = Q_c \rho \pi R^5 \Omega^3 = 1.815 \Omega^3 Q_c \text{ (ft.lbs/sec).}$$

The R.P.M. corresponding to each condition was obtained by assuming a straight line relationship between power and R.P.M. for the full throttle power curve. This amounts to assuming constant torque at full throttle with any blade or flap setting. Therefore, the torque at point O equals the torque at point 1 in the figure below, and

$$Q_c \rho \pi R^5 \Omega^2 = Q_{c_0} \rho \pi R^5 \Omega_0^2$$



therefore

$$\Omega^2 = \Omega_0^2 \frac{Q_{c0}}{Q_c}$$

where

$$Q_{c0} = .001710 \text{ (torque coefficient at design } \lambda = .23)$$

$$\Omega_0^2 = 71240 \text{ (rad/sec)}^2 \text{ corresponding to rated R.P.M. of 2550}$$

$$\Omega = \text{rotational speed corresponding to any other torque coefficient, } Q_c.$$

Using this new Ω the power absorbed can be calculated from the above power formula.

The results of these calculations are tabulated in TABLE X which also shows the per cent of normal power absorbed by the propeller under the various conditions.

Fig. 9 is a plot of the values in TABLE XI and presents the results of TABLE X in non-dimensional form. Fig. 9 shows the per cent of fixed-pitch propeller static thrust versus the per cent of normal R.P.M. or power absorbed to secure this thrust.

A clearer picture of these final results may be had from the table

below which compares the increase in thrust that can be secured with the "flapped" propeller with the increase in thrust of the variable-pitch propeller. The flap angle and blade angle in the respective cases were set to give rated full-power absorption.

Propeller	Increase in Static Thrust
Variable Pitch	.300
Flapped	.132

Finally, the percentage increase in thrust that can be realized by equipping the propeller with trailing-edge flaps is $(.132/.300) \times 100 = 44$ per cent as much as can be realized by turning the "unflapped" blade in the hub.

Care must be exercised in generalizing from the above results because of the particular nature of the propeller used for the example. It is felt that the "flapped" propeller would show up more favorably with a flap designed for this specific purpose. The flap on the M-6 airfoil was designed for large angular movement in both the up and down direction. The flap angle needed in this case is small, in the order of 10° , and, therefore, could no doubt be faired in more closely and thus increase the efficiency of the airfoil section.

Conclusions

The following conclusions can be made from a study of the results and Fig. 9:

1. The static thrust of a propeller can be increased by the use

of trailing-edge flaps which reduce the effective pitch and allow the propeller to turn up to higher R.P.M. on the ground.

2. The maximum increase in static thrust obtainable is about 15 per cent. The optimum occurs at the flap setting which will give rated R.P.M. Here the increase is 13.2 per cent which is 44 per cent as much increase as can be obtained with the conventional variable-pitch propeller at the same R.P.M.

3. Little advantage would be gained by increasing the take-off rating of engines equipped with this type of propeller because the thrust curve flattens out very rapidly above rated R.P.M.

References

1. Hartman, Edwin P.: Considerations of the Take-off Problem. U.S.National Advisory Committee for Aeronautics, Technical Notes No.557, February, 1936.
2. Knight, Montgomery: Propulsive Airscrews. Unpublished lecture notes from Aeronautical Engineering course entitled "Propulsive Airscrews", Georgia School of Technology, Atlanta, Georgia.
3. Weick, Fred E.: Propeller Design - A Simple System Based on Model Propeller Test Data. U.S.National Advisory Committee for Aeronautics, Technical Notes No.237, May, 1926.
4. Jacobs, Eastman N.: "Characteristics of Propeller Sections Tested in the Variable-Density Wind Tunnel." (In U.S.National Advisory Committee for Aeronautics, Annual Report, 1927, Technical Report No.259, p.125.)
5. Higgins, George J. and Jacobs, Eastman N.: "The Effect of a Flap and Aileron on the N.A.C.A.-M6 Airfoil Section." (In U.S.National Advisory Committee for Aeronautics, Annual Report, 1927, Technical Report No.260, p.141.)
6. Jacobs, Eastman N. and Abbott, Ira H.: "The N.A.C.A. Variable-Density Wind Tunnel." (In U.S.National Advisory Committee for Aeronautics, Annual Report, 1932, Technical Report No.416, p.305.)
7. Glauert, Hermann: "Airplane Propellers." (In Durand, W.F., Editor, Aerodynamic Theory, Vol.IV, Div.I, p.169, Berlin, Julius Springer, 1936.)

TABLE I

Geometric Characteristics of the Propeller (See Fig. 1a)

Section	Radius (in.)	$x = \frac{r}{R}$	Chord (ins) (See Fig.1)	$C = \frac{c}{\pi r}$	θ°
A	9.0	.25	5.50	.1945	52.5
B	16.2	.45	6.00	.1180	35.8
C	21.6	.60	5.75	.0847	28.5
D	27.0	.75	5.00	.0589	23.4
E	30.6	.85	4.25	.0442	20.9
F	34.2	.95	2.75	.0256	18.9
Tip	36.0	1.00	0.00	.0000	18.0

TABLE II

Propeller Characteristics for Condition 0
(Design - High Speed)

$$\lambda = .23 \quad \theta_{.75} = 23.4^\circ \quad \delta_f = 0$$

Section	θ°	ϕ°	$R \frac{dT_c}{dr}$	$R \frac{dQ_c}{dr}$
A	52.5	51.5	.0004	.00015
B	35.8	30.1	.0064	.00175
C	28.5	22.9	.0101	.00268
D	23.4	18.3	.0121	.00319
E	20.9	16.0	.0125	.00326
F	18.9	14.1	.0099	.00256

TABLE III

Propeller Characteristics for Condition 1
(Design - Static Thrust)

$$\lambda = 0 \quad \theta_{.75} = 23.4^\circ \quad \delta_f = 0$$

Section	θ°	ϕ°	$R \frac{dT_c}{dr}$	$R \frac{dQ_c}{dr}$
A	52.5	21.1	.0020	.00065
B	35.8	13.5	.0112	.00253
C	28.5	10.5	.0238	.00376
D	23.4	8.2	.0325	.00433
E	20.9	6.8	.0340	.00408
F	18.9	5.1	.0237	.00255

TABLE IV

Propeller Characteristics for Condition 2
Variable Pitch - Static Thrust

$\lambda = 0$ $\Theta_{.75} = 23.4 - 5^* = 18.4^\circ$ $\delta_f = 0$

Section	Θ°	ϕ°	$R \frac{dT_c}{dr}$	$R \frac{dQ_c}{dr}$
A	47.5	19.8	.0023	.00050
B	30.8	12.5	.0140	.00197
C	23.5	9.3	.0231	.00258
D	18.4	7.0	.0258	.00271
E	15.9	5.7	.0253	.00249
F	13.9	4.2	.0196	.00166

TABLE V

Propeller Characteristics for Condition 3
Variable Pitch - Static Thrust

$\lambda = 0$ $\Theta_{.75} = 23.4 - 10 = 13.4^\circ$ $\delta_f = 0$

Section	Θ°	ϕ°	$R \frac{dT_c}{dr}$	$R \frac{dQ_c}{dr}$
A	42.5	18.5	.0029	.00046
B	25.8	11.2	.0138	.00138
C	18.5	8.0	.0176	.00166
D	13.4	5.7	.0177	.00153
E	10.9	4.5	.0160	.00129
F	8.9	3.2	.0116	.00080

TABLE VI

Propeller Characteristics for Condition 4
"Flapped" Blade - Static Thrust

$\lambda = 0$ $\Theta_{.75} = 23.4 - 2.8 = 20.6^\circ$ $\delta_f = -5^\circ$

Section	Θ°	ϕ°	$R \frac{dT_c}{dr}$	$R \frac{dQ_c}{dr}$
A	49.7	20.4	.00200	.00057
B	33.0	13.1	.01078	.00227
C	25.7	9.8	.02155	.00332
D	20.6	7.5	.02915	.00348
E	18.1	6.2	.02980	.00333
F	16.1	4.6	.02330	.00226

TABLE VII

Propeller Characteristics for Condition 5
"Flapped" Blade - Static Thrust

$\lambda = 0$ $\theta_{.75} = 23.4 - 4.9 = 18.5^\circ$ $\delta_f = -10^\circ$

Section	θ°	ϕ°	$R \frac{dT_c}{dr}$	$R \frac{dQ_c}{dr}$
A	47.6	19.8	.00172	.00053
B	30.9	12.5	.00994	.00204
C	23.6	9.4	.01980	.00288
D	18.5	7.0	.02590	.00296
E	16.0	5.8	.02570	.00276
F	14.0	4.3	.01970	.00186

TABLE VIII

Propeller Characteristics for Condition 6
"Flapped" Blade - Static Thrust

$\lambda = 0$ $\theta_{.75} = 23.4 - 7.5 = 15.9^\circ$ $\delta_f = -20^\circ$

Section	θ°	ϕ°	$R \frac{dT_c}{dr}$	$R \frac{dQ_c}{dr}$
A	45.0	19.1	.00143	.00042
B	28.3	11.9	.00815	.00157
C	21.0	8.7	.01550	.00219
D	15.9	6.4	.01895	.00215
E	13.4	5.2	.01820	.00195
F	11.4	3.8	.01351	.00132

TABLE IX

Determination of Thrust and Torque Coefficient

Condition	$R \frac{dT_c}{dQ_c}$ (sq. in.)	T_c	$R \frac{dQ_c}{dr}$ (sq. in.)	Q_c
0	3.21	.00642	8.55	.001710
1	7.83	.01566	11.71	.002342
2	7.03	.01406	7.95	.001590
3	5.28	.01056	4.99	.000998
4	7.14	.01428	9.98	.001996
5	6.39	.01278	8.63	.001726
6	4.81	.00962	6.41	.001282

TABLE X

Determination of Thrust and Power

Cond.	Q_c	T_c	$\Omega^2 \frac{121.8}{Q_c}$	Ω (Rad/ sec)	T (lbs)	P (ft.lbs /sec)	Per cent of Normal P
0	.001710	.00642	71240	266.9	276.5	59000	100.0
1	.002342	.01566	51950	228.0	482.0	50300	85.2
2	.001590	.01406	76600	276.5	651.0	61050	103.4
3	.000998	.01056	12200	349.3	736.0	77200	131.0
4	.001996	.01428	61050	247.0	527.0	54600	92.5
5	.001726	.01278	70610	265.5	545.0	58650	99.4
6	.001282	.00962	94900	308.0	552.5	68000	115.2

TABLE XI

Static Thrust and R.P.M. Comparison

Condition	T	ΔT (T - T ₁)	$\frac{T}{T_1}$	R.P.M.	$\frac{R.P.M.}{2550}$
0	276	- 206	.573	2550	1
1	482	0	1.000	2178	.853
2	651	169	1.350	2648	1.038
3	736	254	1.527	3336	1.317
4	527	45	1.093	2364	.926
5	545	63	1.130	2538	.995
6	552	70	1.145	2946	1.155

FIG. 1

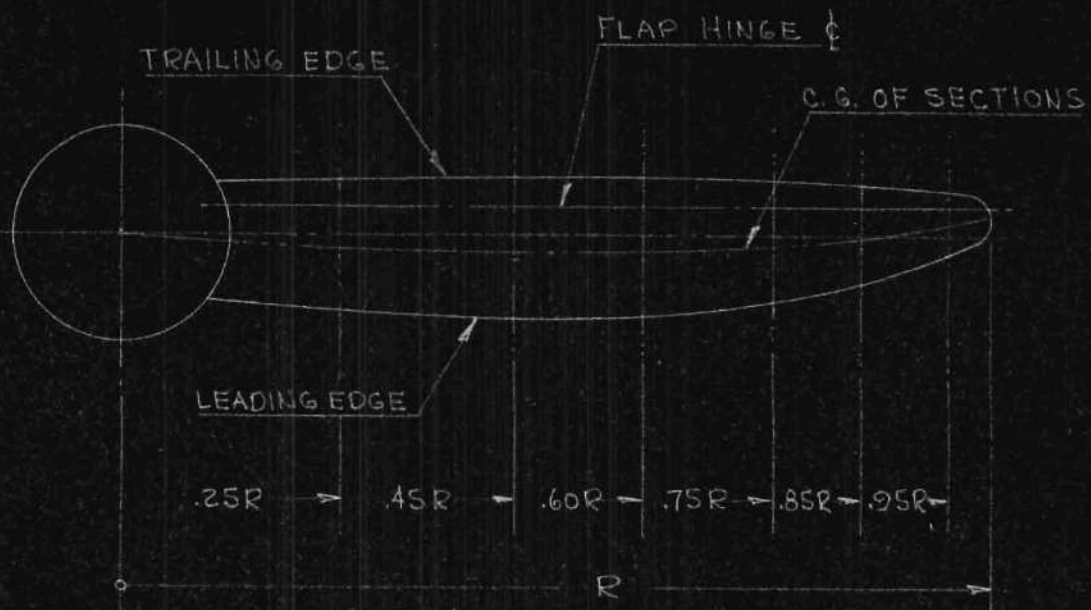


FIG. 1. a. BLADE PLAN FORM

$\alpha_0 =$ ABSOLUTE ANGLE OF ATTACK

$\alpha_3 =$ GEOMETRICAL ANGLE OF ATTACK



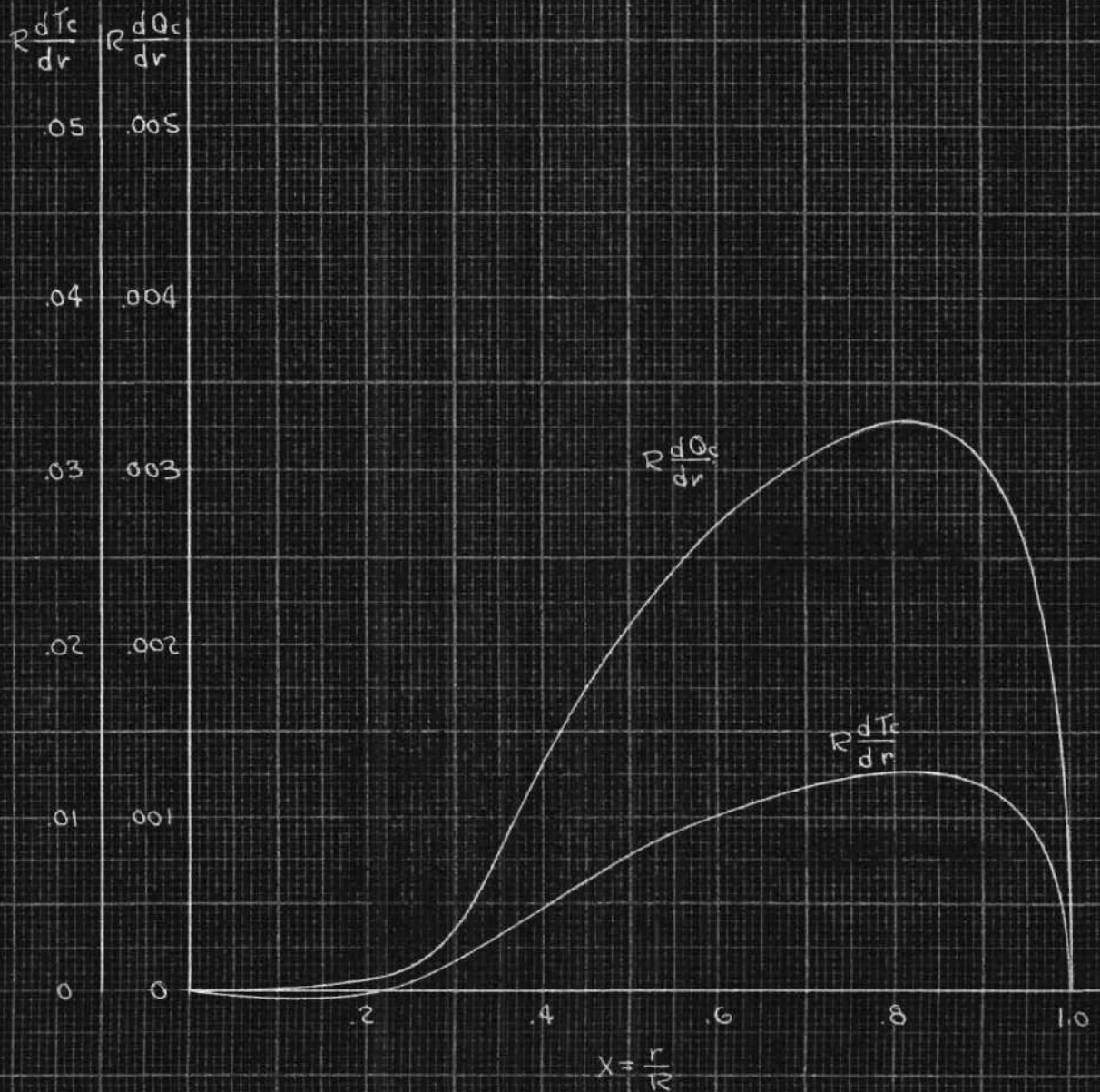
FIG. 1. b. BLADE SECTION AT $\frac{3}{4}$ RADIUS (M-G AIRFOIL SECTION) SHOWING 20% PLAIN FLAP.

FIG. 2-THRUST & TORQUE GRADING CURVES FOR
CONDITION 0 (Fixed Pitch)

$\lambda = .23$ (Design High Speed)

Blade Twisted in Hub 0°

Flop Angle, $\delta_f = 0^\circ$



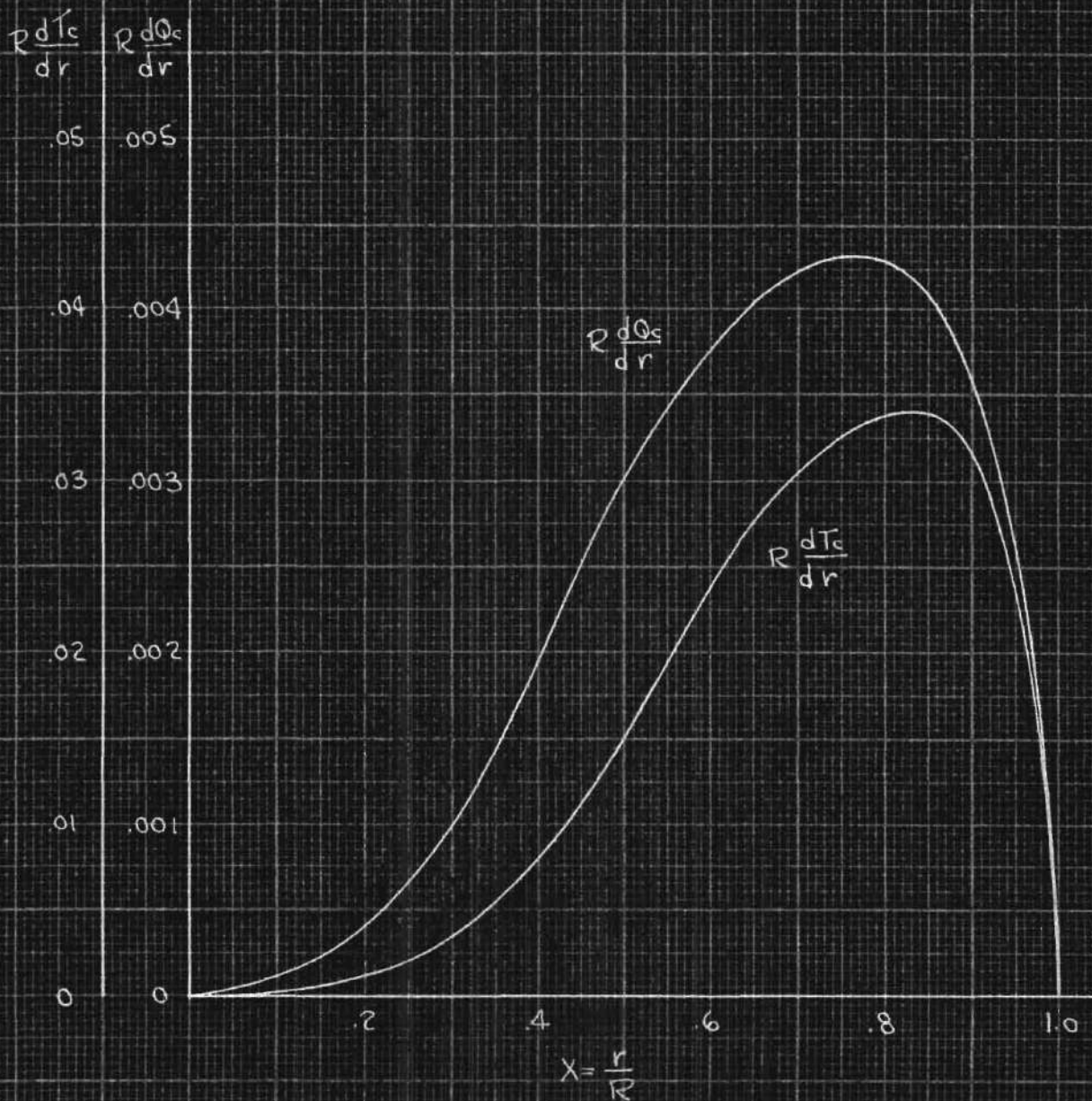
D.W.D
 4-15-40

FIG. 3- THRUST & TORQUE GRADING CURVES FOR
CONDITION 1 (Fixed Pitch)

$$\lambda = 0$$

Blade Twisted in Hub 0°

Flap Angle, $\delta_f = 0^\circ$



D.W.D.
 4-2-90

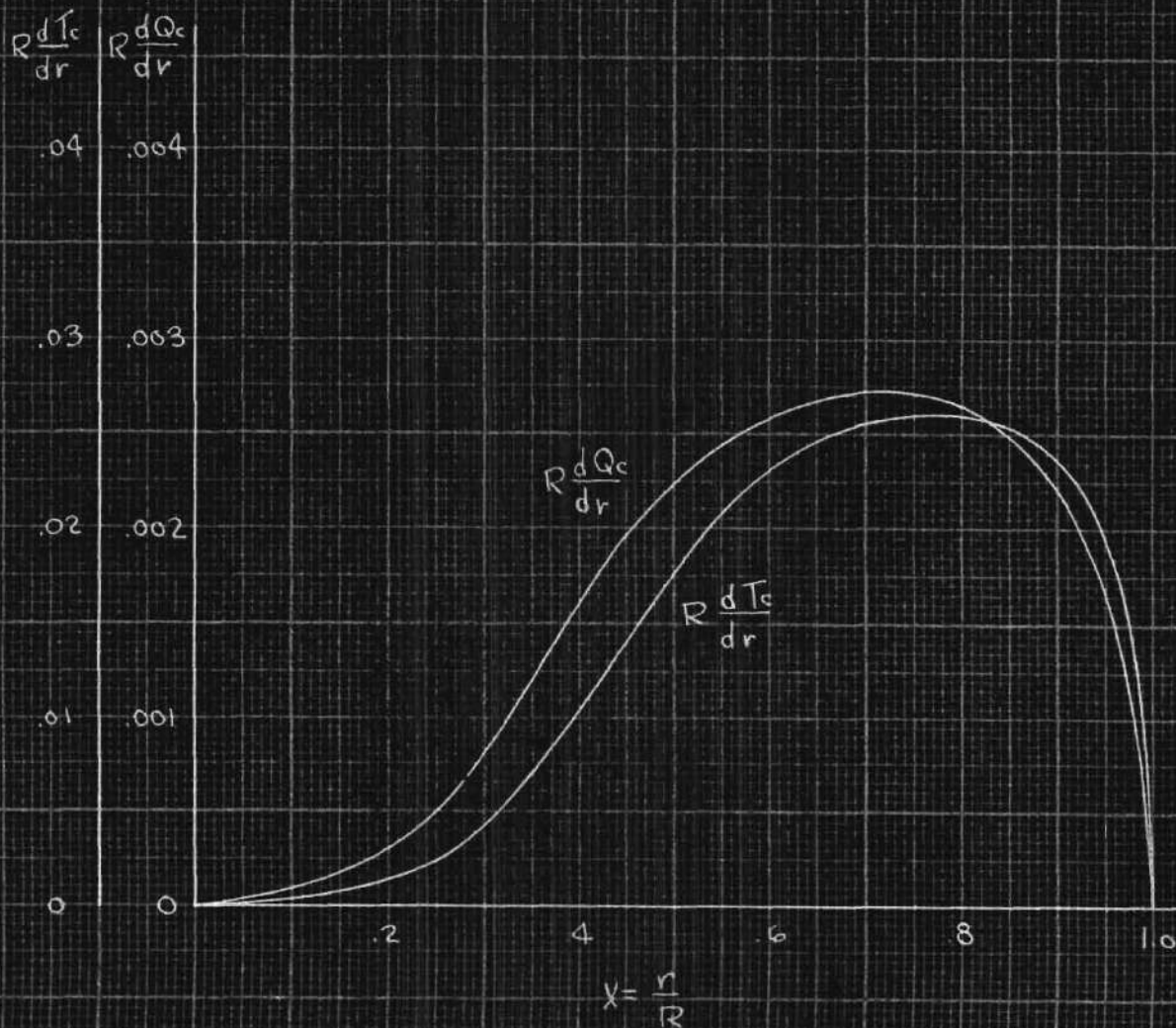
FIG. 4 - THRUST & TORQUE GRADING CURVES FOR

COND. 2 (Var Pitch)

$$\lambda = 0$$

Blade Twisted in Hub -5°

Flop Angle, $\delta_f = 0$



D.W.D.
4-7-40

FIG 5 - THRUST & TORQUE GRADING CURVES FOR

COND. 3 (Var. Pitch)

$\lambda = 0$

Blade Twisted in Hub -10°

Flap Angle, $\delta_f = 0^\circ$

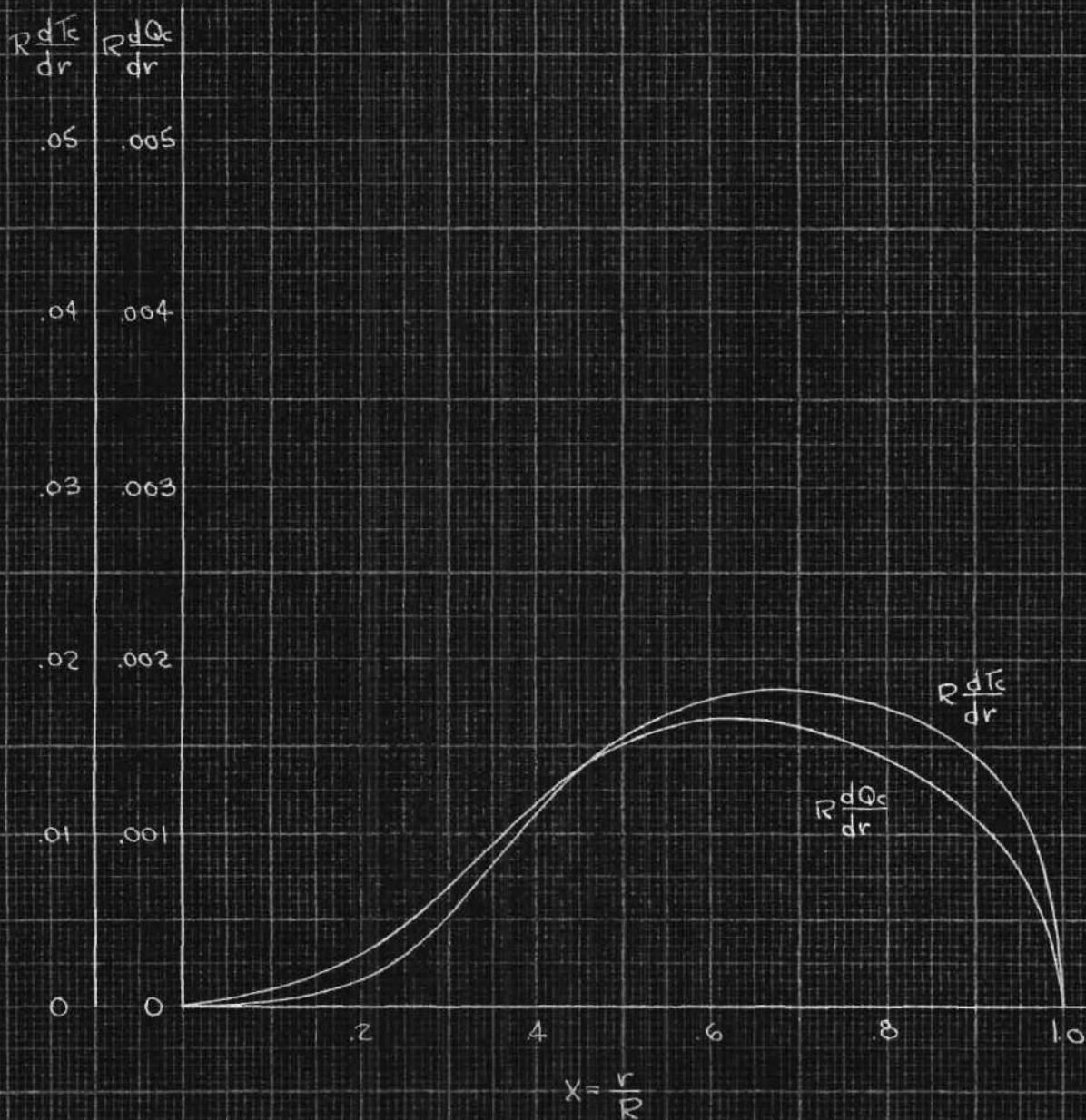


FIG. 6. THRUST & TORQUE GRADING CURVES FOR

COND. 4: (Flapped Blade)

$$\lambda = 0$$

Blade Twisted in Hub 0°

Flop Angle, $\delta_f = -5^\circ$

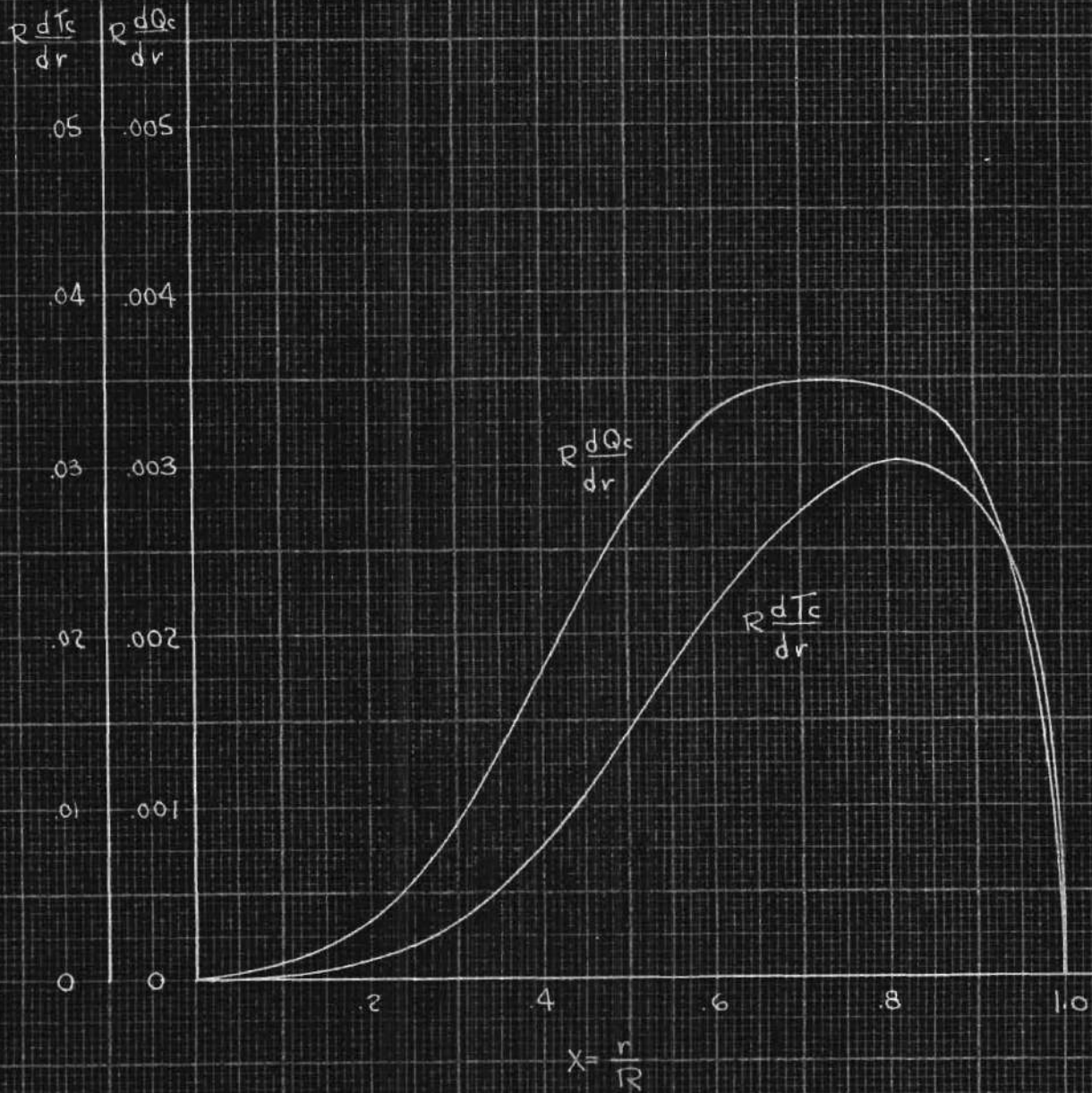


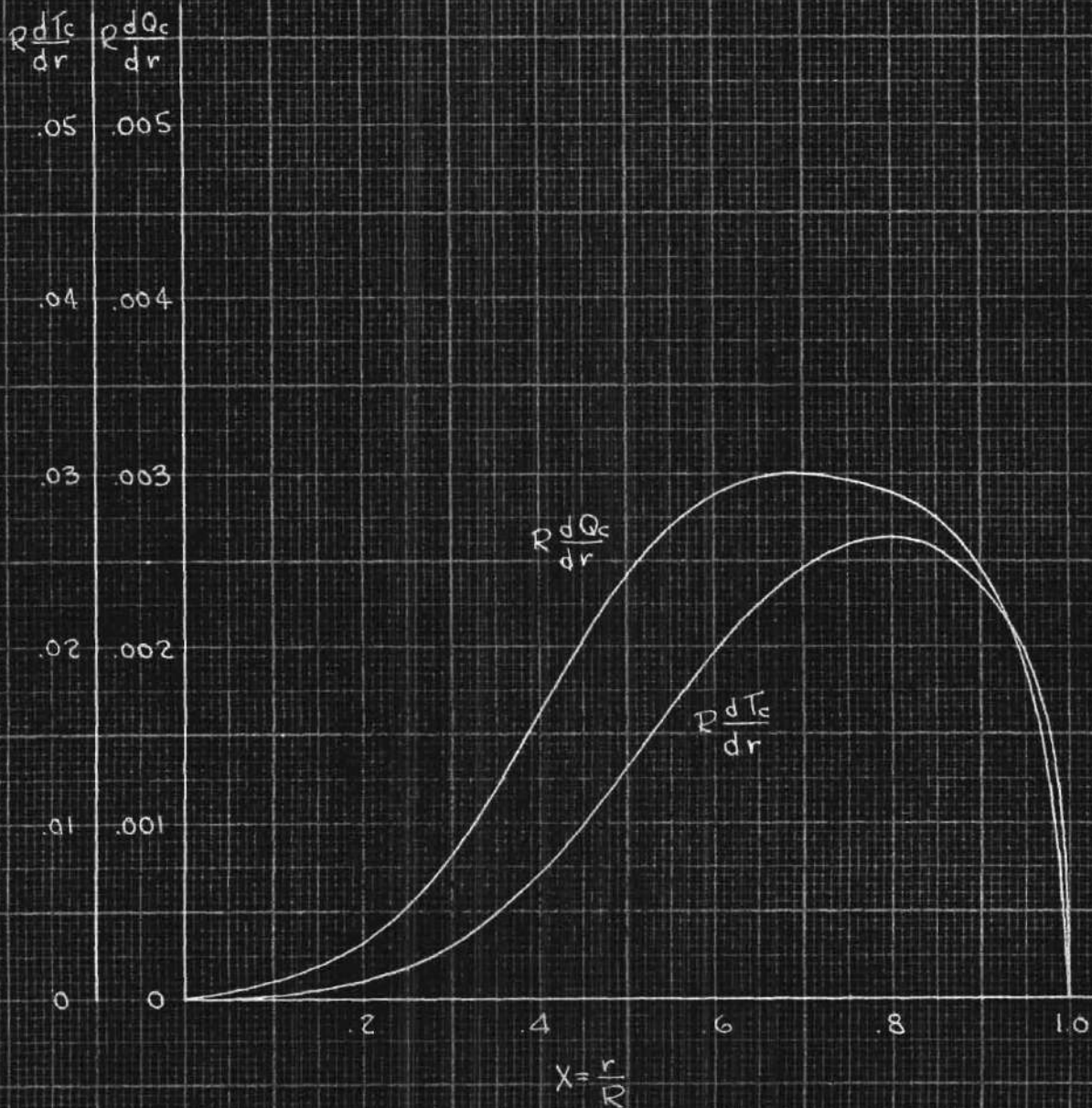
FIG. 7-THRUST & TORQUE GRADING CURVES FOR

COND. 5 (Flapped Blade)

$$\lambda = 0$$

Blade Twisted in Hub 0°

Flap Angle, $\delta_f = -10^\circ$



D.W.D
4-13-40

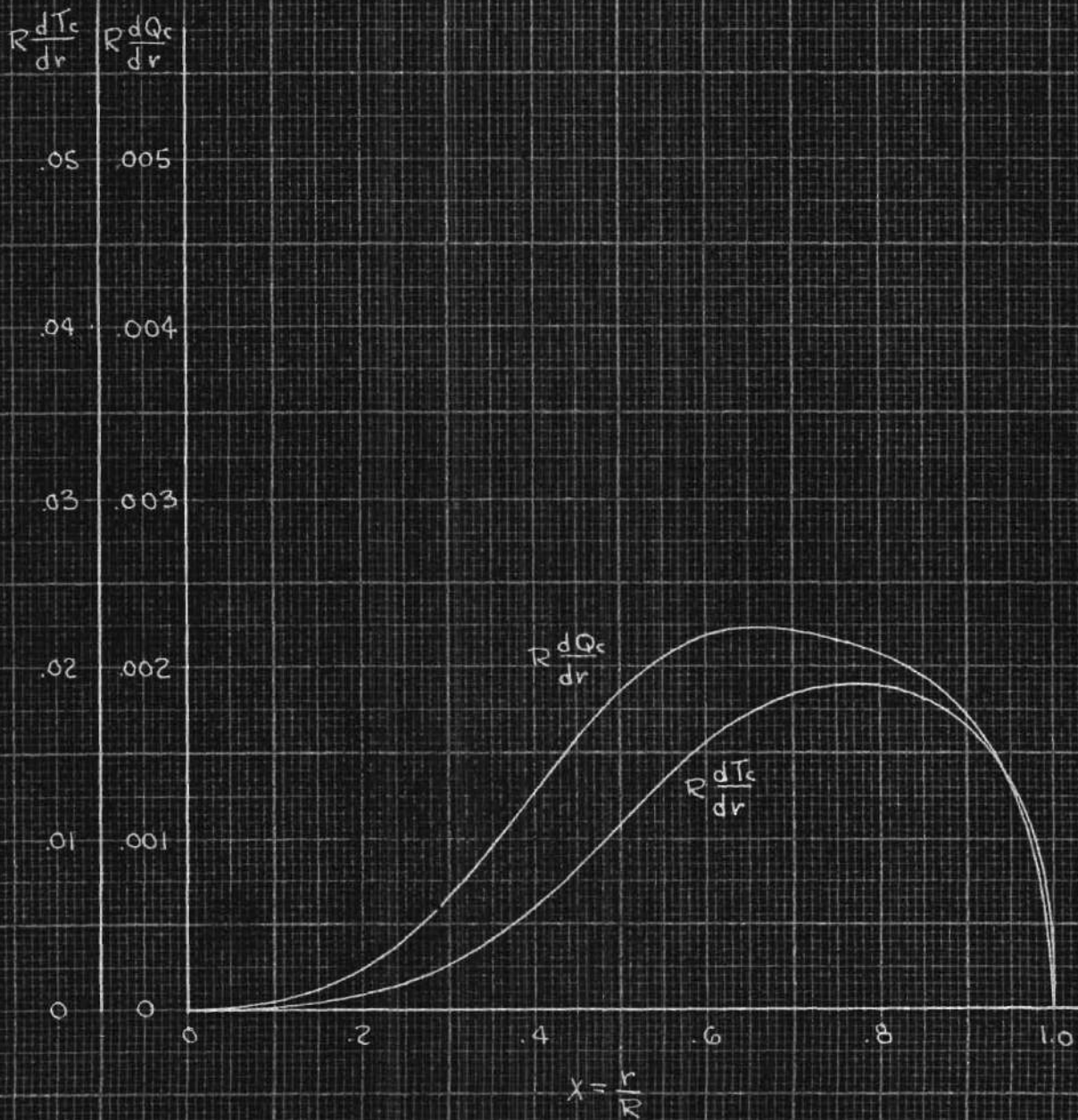
FIG. 8.- THRUST & TORQUE GRADING CURVES FOR

COND 6 (Flapped Blade)

$$\lambda = 0$$

Blade Twisted in Hub 0°

Flap Angle, $\delta_f = -20^\circ$



D.W.D.
4-15-40

FIG. 9 - PERCENT OF RATED R.P.M. VS. PERCENT OF FIXED PITCH STATIC THRUST FOR VARIABLE PITCH AND "FLAPPED" PROPELLER

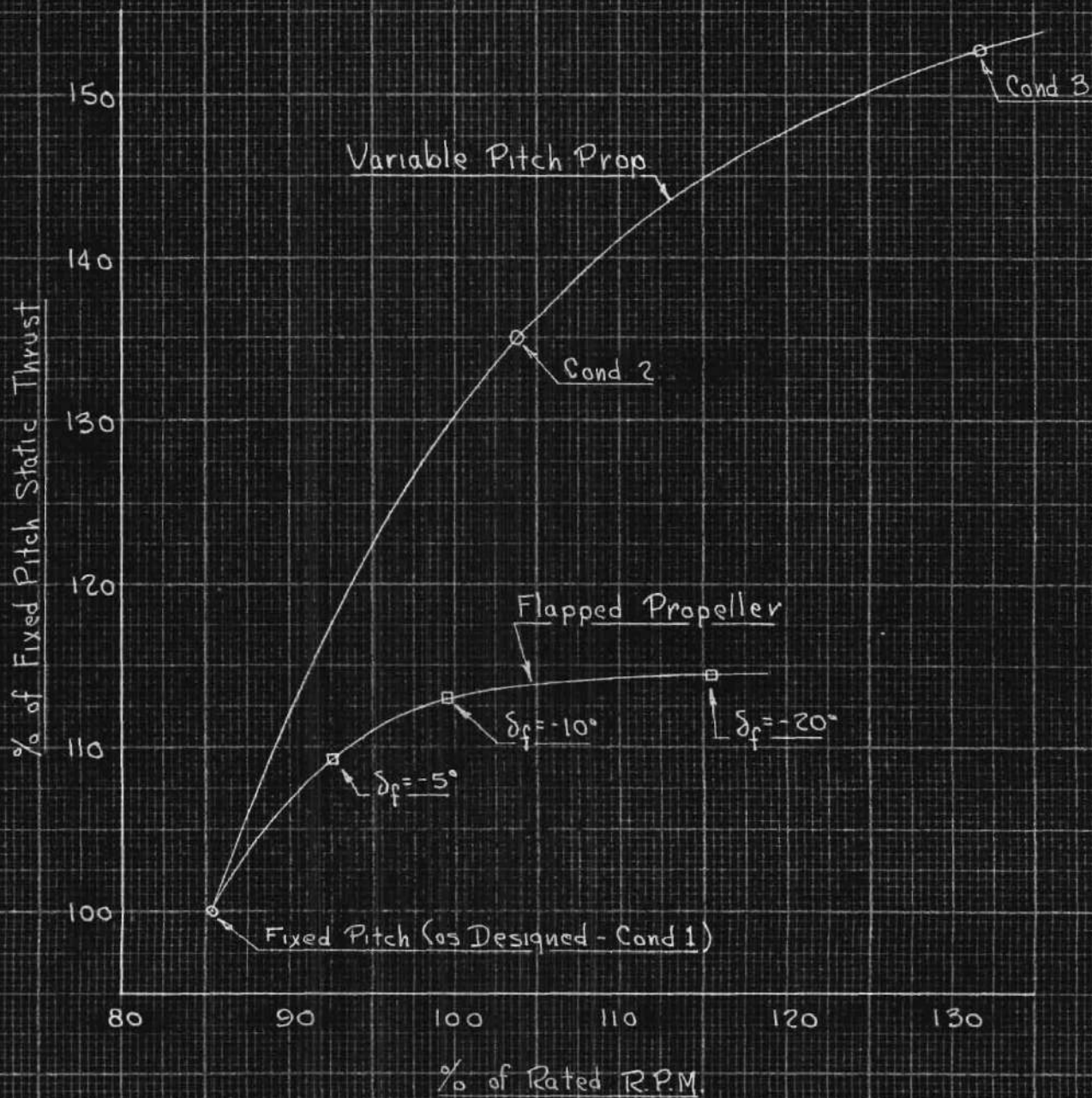


FIG. 10- LIFT COEFFICIENT VERSUS ANGLE OF ATTACK
FOR INFINITE ASPECT RATIO OF N.A.C.A.-M6
AIRFOIL WITH DIFFERENT FLAP SETTINGS
OF A 20 PERCENT CHORD FLAP

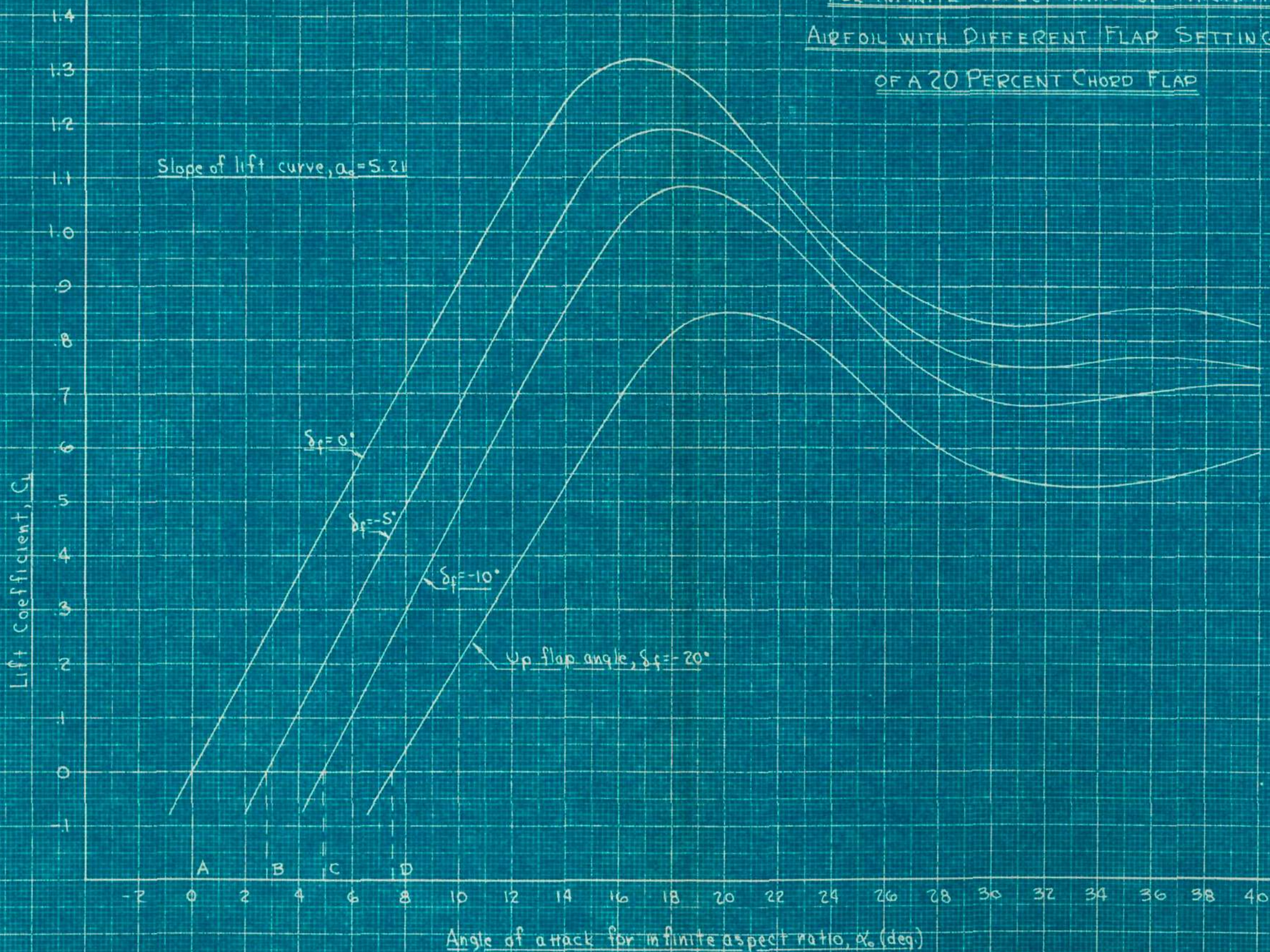


FIG. 11 - PROFILE DRAG COEFFICIENT VERSUS ANGLE OF ATTACK FOR INFINITE ASPECT RATIO OF NACA M-6 AIRFOIL WITH DIFFERENT FLAP SETTINGS OF A 20 PERCENT CHORD FLAP

